Percolation and jamming in random sequential adsorption of linear segments on a square lattice

Grzegorz Kondrat* and Andrzej Pękalski†

Institute of Theoretical Physics, University of Wrocław, pl. M. Borna 9, 50-204 Wrocław, Poland

We present the results of a study of random sequential adsorption of linear segments (needles) on sites of a square lattice. We show that the percolation threshold is a nonmonotonic function of the length of the adsorbed needle, showing a minimum for a certain length of the needles, while the jamming threshold decreases to a constant with a power law. The ratio of the two thresholds is also nonmonotonic and it remains constant only in a restricted range of the needles length. We determine the values of the correlation length exponent for percolation, jamming, and their ratio.

PACS number(s): 05.40.−a, 64.60.Ak

I. INTRODUCTION

The problem of percolation is an old one [1] but still new results appear and some unsolved questions remain [2]. In general site percolation is defined on a d-dimensional lattice where each site can be either occupied with the probability c or empty with the probability $1-c$. Neighboring occupied sites form a cluster. If it is so large that it reaches the two opposite edges of the lattice, e.g., top and bottom, the cluster is said to be percolating. The lowest concentration of occupied sites for which there is a percolating (or spanning) cluster for an infinite lattice is called the percolation threshold c_p [2].

Another realization of the percolation problem is random sequential adsorption (RSA), in which objects (point particles, segments, rectangles, etc.) are put on randomly chosen sites and the objects do not move [3]. It is also possible to consider RSA in a continuum [4].

Jamming is a problem related to RSA percolation [3]. Again objects are placed randomly on the lattice sites until a concentration c_j is reached, where there is no room on the lattice for the next object. For pointlike particles $c_j = 1$, but for spatially extended entities $c_j < 1$. Continuum models of jamming also exist [3].

The RSA models irreversible dissociation [5] and binding of large ligands to polymer chains [6]. Another area of applicability is the deposition of large molecules on solid surfaces, like proteins [7] or macromolecules on biological membranes [8]. The isotropic-nematic transition in the hard rods such as polymers, has been studied first by Flory [9] and later, e.g., in Ref. [10]. Spatial organization of needles into a well-organized nematic phase is however a different problem, not considered here. General forms of percolation models have a wide range of applications—from chemisorption, spatially disordered systems, porous materials, car parking, and ecology [3], to separating the good and bad people at the entrance to Hades [11]. For overview of percolation, jamming, and related problems see Ref. [3].

In a recently published paper [12] Vanderwalle *et al.* studied the relation between the two transitions—percolation and jamming. They used two kinds of objects—linear segments of length 2 to 10 and square blocks. They have found that the ratio of the two threshold concentrations c_p and c_j is constant $c_p/c_j \approx 0.62$, regardless of the length of the needle.

In the present paper we extend the study of Vanderwalle *et al.* to larger lattices and longer objects (we consider only linear segments). In particular we shall check the claim that the c_p/c_j ratio does not depend on the length of the needles.

II. MODEL

We consider a square lattice of size $L \times L$. On the sites of the lattice we put randomly linear segments (needles) of a given length a, with the constraint that the needles cannot cross each other, although they may touch themselves. We used hard boundary conditions, i.e., the needles may touch the edge of the lattice but they cannot stick out of it—each needle must lay totally inside the lattice. Adopting open boundary conditions does not affect the results.

To achieve simulation efficiency, our algorithm of deposition needles consists of two parts designed for two different regimes. First when the current concentration of the needles is small, we chose randomly, from a uniform distribution, the orientation (vertical or horizontal) and position of the upper left end of the needle to be inserted. If there is enough space on the lattice, the needle is deposited, if not, we pass to the next try. After a certain number of adsorption trials we switch to the other regime where the dense routine is applied. A list of all empty sites and orientations still available is made. From that list a site is randomly chosen. We determine the direction of the needle and check whether the needle can be put there. In any case the site is removed from the list. The process is continued untill the last item on the list. Such organization saves time, since we avoid inserting needles into densely packed regions.

A cluster is defined as a group of sites linked by the needles. If there is an uninterrupted path between the top and the bottom of the lattice, the cluster is said to be percolating or spanning, and the concentration of occupied sites defines the percolation threshold c_p. The concentration at which no more needles could be put on the lattice without violating the constraint determines the jamming threshold c_j.

We have considered lattices of sizes $L = 30$, 100, 300, 1000, 2500 and needles of length $a = 1, \ldots, 2000$. On the
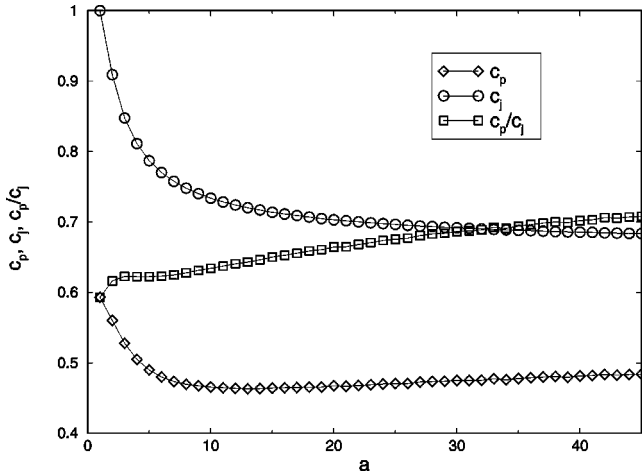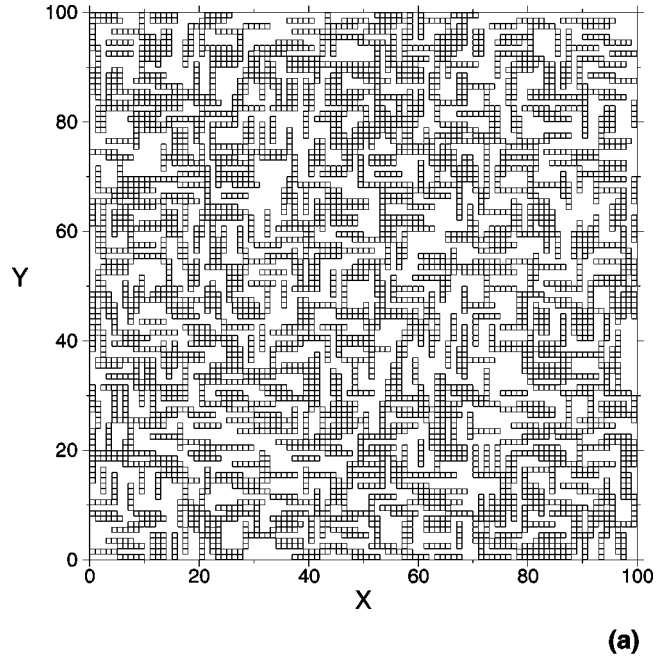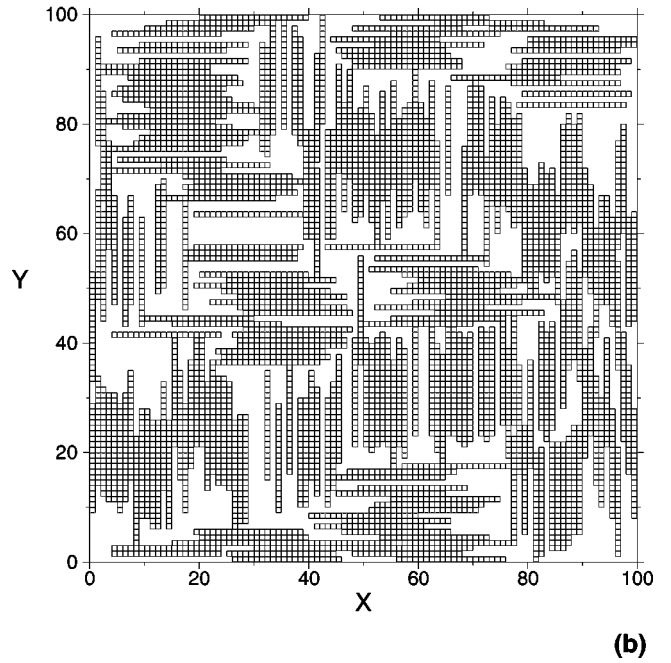
FIG. 1. Thresholds for percolation c_p, jamming c_j, and their ratio c_p/c_j vs needles' length a. Lattice size $L=2500$. Averaged over 100 samples. The x axis is in arb. units in all figures.

FIG. 2. Percolation threshold c_p vs needles' length a. $L=2500$, 100 runs. (a) Short needles $a=1,\ldots,45$; (b) long needles $a=1,\ldots,2000$.
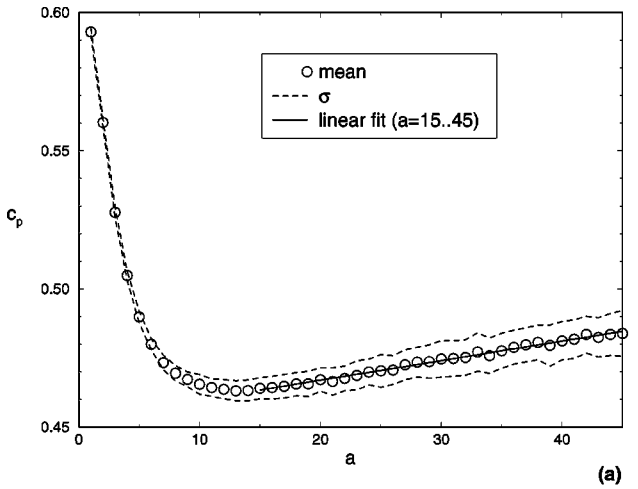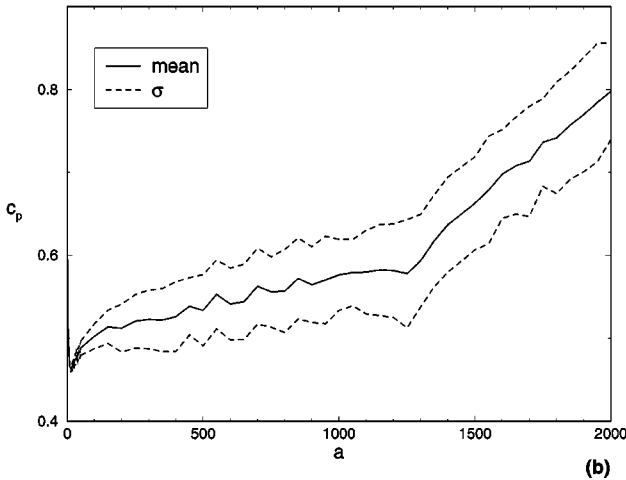
(a)

(b)

FIG. 3. Snapshot of a spatial distribution of needles at the percolation threshold for $L=100$. (a) $a=5$, (b) $a=20$. The y axes are in arb. units.

smallest lattices only smaller needles were located. Averaging was done over 100 independent runs. We have checked that averaging over 1000 runs did not reduce the error (mean standard deviation - σ) in a marked way.

III. RESULTS

Our main results of the simulations are presented in Fig. 1, where the percolation and jamming thresholds, as well as their ratio, are plotted against the length of the needles (a
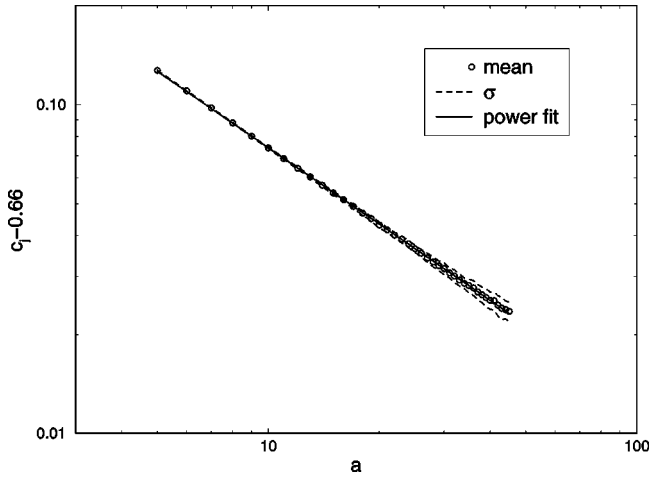
FIG. 4. Jamming threshold c_j vs needles' length a on a log–log plot. $L=2500$, 100 runs. $a=5,\ldots,45$.

FIG. 6. Percolation to jamming thresholds ratio c_p/c_j vs needles' length a. $L=2500$, 100 runs. $a=1,\ldots,2000$.

$=1,\ldots,45)$. These data are obtained for lattice size $L=2500$. As convergence and error analysis shows (see below) we can safely accept them as the asymptotic ($L\rightarrow\infty$) values.

The percolation threshold for $a=1,\ldots,13$ diminishes, then it begins to grow linearly with the slope 0.000 71. The minimum value $c_{p\min}=0.463$ is reached for $a=13$. As seen in Fig. 2, the σ increases with the size of the needles starting from $0.001(a=1)$ up to $0.008(a=45)$. The increase of the percolation threshold for longer a is however quite clear. The appearance of this unexpected feature is connected with the condition that the needles may touch themselves but they cannot cross. In the simulations where the restriction has been lifted we observed no minimum but a monotonic decrease. In the model considered here the needles have the tendency to align in parallel not only with respect to the edges of the lattice but also to themselves (see Fig. 3); hence the needles form compact clusters. In the case of horizontally oriented needles, in order to move, e.g., two steps down, two
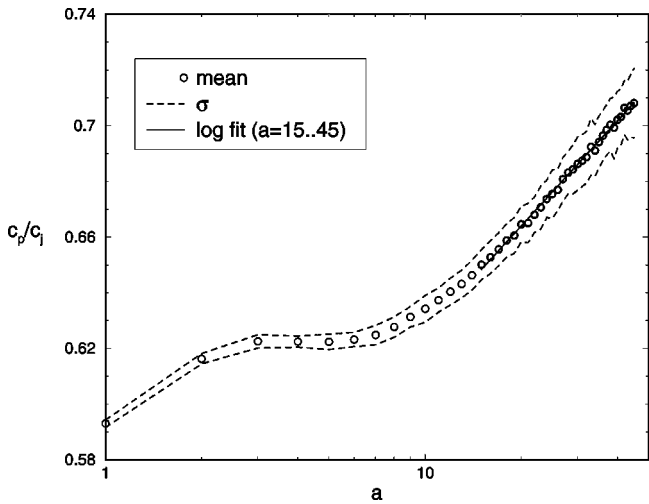

FIG. 5. Percolation to jamming thresholds ratio c_p/c_j vs needles' length a. $L=2500$, 100 runs. Logaritmic fit for $a=15,\ldots,45$.
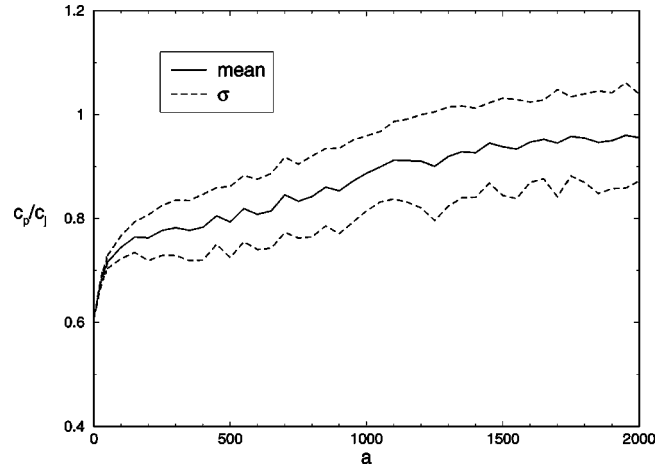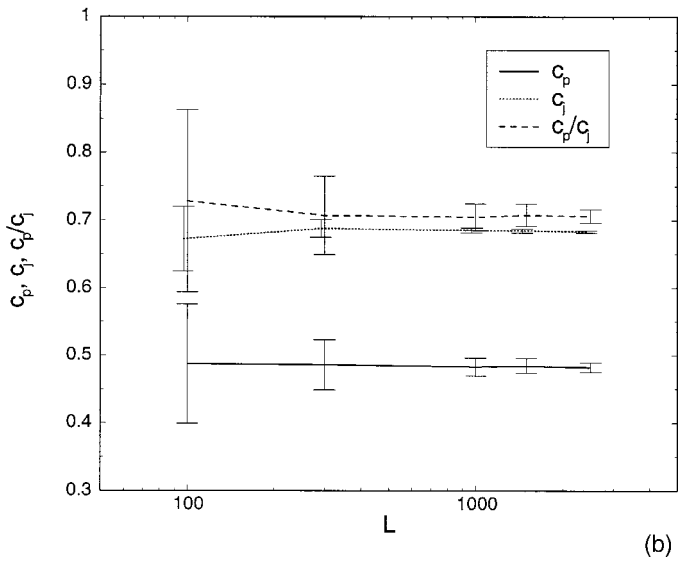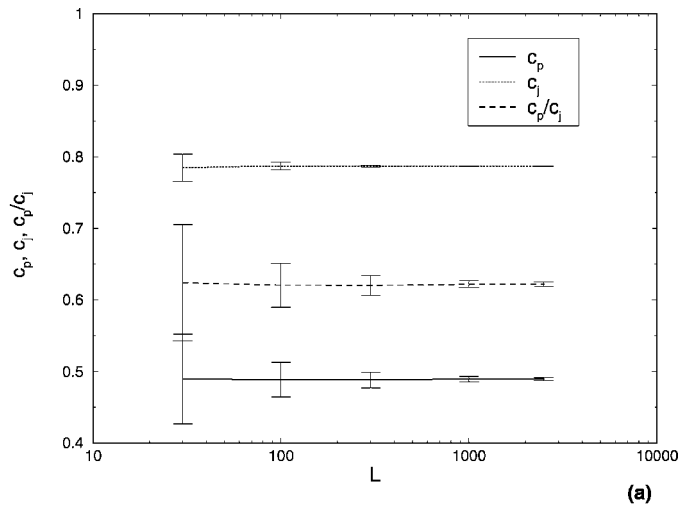

FIG. 7. Convergence analysis of percolation c_p, jamming thresholds c_j, and their ratio c_p/c_j, vs lattice size L. 100 runs. (a) $a=5$, (b) $a=45$.
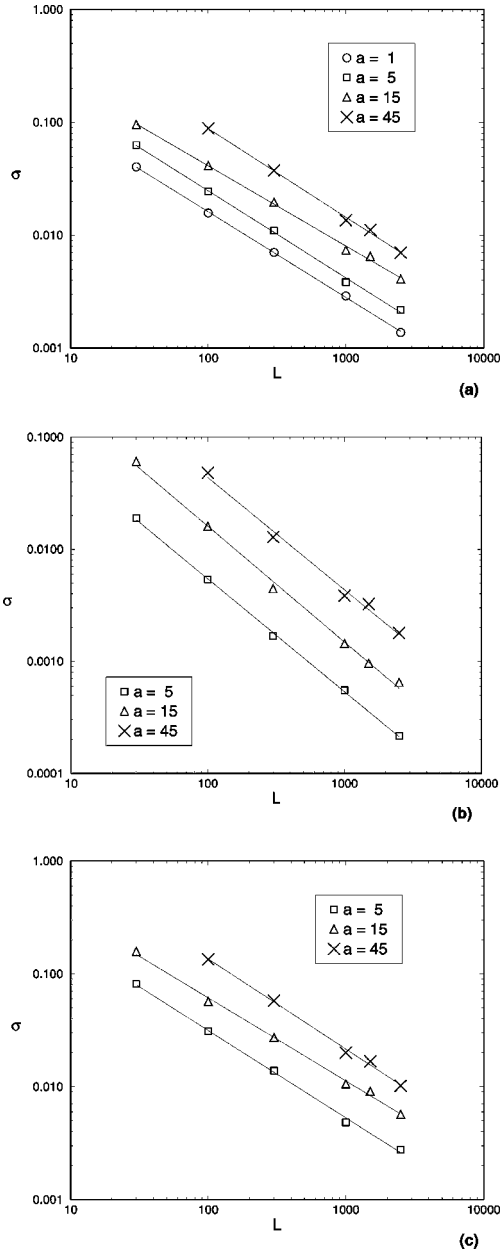
(a)

(b)

(c)

FIG. 8. Deviation analysis. σ vs lattice size L for several values of the needles' length. (a) Percolation, (b) jamming, and (c) percolation to jamming ratio.
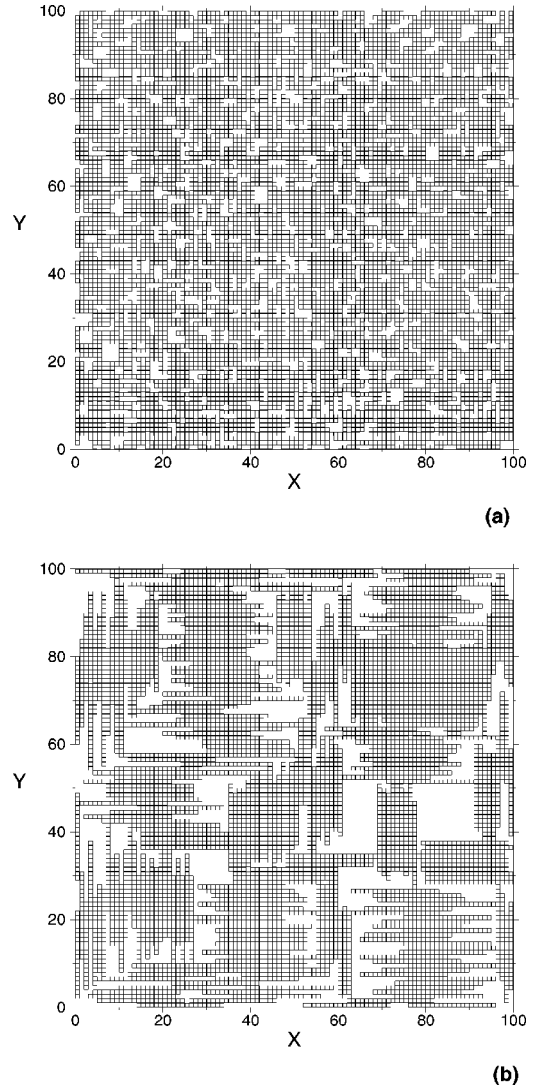

(a)

(b)

FIG. 9. Snapshot of a spatial distribution of needles at the jamming threshold for $L=100$. (a) $a=5$, (b) $a=20$. The y axes are in arb. units.

$$c_j = c_j^* + 0.44a^{-0.77}. \qquad (1)$$

The uncertainty of the exponent derived from the graph analysis equals 0.02. Clearly this behavior differs essentially from bare power law postulated in Ref. [4]:

$$c_j \sim a^{-0.2}, \qquad (2)$$

for the continuum (off-lattice) case of RSA of randomly oriented and highly anisotropic (length to wide) rectangles. Their a coincides with our length of needles a. In the discrete case we did not observe the maximum of c_j at $a=2$ reported in Ref. [4]. The reason is that on the lattice the number of possible orientations of the needles is restricted to $z/2$ (where z is the coordination number of the lattice) in contrast to the continuum case. It is interesting that the asymptotic concentration for jamming (for $a \to \infty$) is 0 off lattice and it remains finite in the discrete case.

needles of length a are needed. The longer are the needles the higher is the percentage of occupied sites necessary for passing these two steps. The increase of $c_p(a)$ is to a certain degree compensated by vertically oriented needles, which however also form clusters, thus offering many equivalent ways for percolation. Further simulations for much longer needles indicate continuous increase in c_p, although at a slower rate—see Fig. 2(b). The jamming thresholds obtained from the simulations have much smaller error than that for percolation and even for $a=45$ it is below 0.002. Values of c_j, as a function of a, decrease according to a power law (very good fit for all $a \geqslant 5$) approaching the asymptotic value $c_j^* = 0.66 \pm 0.01$ (see Fig. 4):

Another interesting quantity in our model is the ratio c_p/c_j as a function of a (see Fig. 5). It grows for $a = 1,\ldots,3$, then it stabilizes untill $a=7$ and then it grows again. The plateau value of $c_p/c_j \approx 0.62$, the constant found in Ref. [12]. The growth for longer needles $(15 \leqslant a \leqslant 45)$ could be fitted by a logarithmic dependence

$$c_p/c_j \sim 0.50 + 0.13 \log a. \tag{3}$$

Further simulations for longer needles (see Fig. 6) support our claim of monotonic increase in c_p/c_j over a wide range of a (even up to $a=2000$). We may conclude therefore that the universality claimed in Ref. [12] holds only in a rather restricted range of $a \in [3,7]$. As a matter of fact, the value of c_p/c_j for $a>7$ shown in Table I of Ref. [12] is greater than those for $a \leqslant 7$ but the authors attribute it to the finite-size effects. This is however most probably just the beginning of the growth of c_p/c_j.

We analyzed the dependence of the obtained thresholds on the lattice size L and needles' length a focusing on convergence. It appeared that for the ratio $a/L < 1/3$ the values of c_p and c_j do not vary much with increasing L (keeping a constant)—see Figs. 7(a) and 7(b). The error bars (here σ) however decrease rapidly with L, while the difference of the thresholds for different lattice sizes is much smaller than the appropriate error. Thus it is safe to take the values of the thresholds from the simulations with $L=2500$ as the asymptotic (exact) ones.

The finite-size effects can clearly be seen in Fig. 2(b), where c_p is drawn against $a=1,\ldots,2000$ for $L=2500$. At $a=L/2$ we can notice a sharp change in the slope of the function $c_p(a)$.

Consider now the dependence of σ of $c_p, c_j, c_p/c_j$ on the lattice size. σ is analogous to the quantity Δ defined in Ref. [12] as the sharpness of the transition (nonpercolating to percolating or nonjammed to jammed). Here however the power-law approach to the asymptotic value $p(\infty) - p(L) \sim L^{-1/\nu}$ [cf. formula (3) in Ref. [12]] does not hold. We have found (see Fig. 8) that the σ for percolation (Δ_p), jamming (Δ_j), and the c_p/c_j ratio (Δ_r) decrease with the lattice size according to the power laws

$$\Delta_p \sim L^{-1/\nu_p}, \quad 1/\nu_p = 0.75 \pm 0.05,$$

$$\Delta_j \sim L^{-1/\nu_j}, \quad 1/\nu_j = 1.00 \pm 0.05,$$

$$\Delta_r \sim L^{-1/\nu_r}, \quad 1/\nu_r = 0.77 \pm 0.05. \tag{4}$$

Here ν corresponds to the correlation length exponent [2]

$$\xi \sim |c - c_p|^{-\nu}. \tag{5}$$

These values are, within the error bars, the same for all $a = 1,\ldots,45$ and agree with those found by Vanderwalle *et al.* [12] Also Nakamura [13] found $\nu_j = 1.0 \pm 0.1$ for RSA of square blocks. It seems therefore that the exponents ν are good candidates for universal quantities.

Examples of spatial arrangements of shorter $(a=5)$ and longer $(a=20)$ needles on a lattice 100×100 are shown in Figs. 3 (percolation) and 9 (jamming). Analysis based on examination of different runs shows some regularity in the needles distribution—we have found that the needles near the edges have the tendency to stick along the borders. Longer needles, for obvious reasons, form clusters of parallel alignment, as was already observed in Ref. [12].

IV. CONCLUSIONS

We have performed extensive simulations of RSA using linear segments of size $a=1,\ldots,45$ on square lattice sites. We have found that the percolation threshold is a nonmonotonic function of a, having a minimum due to parallel orientation of the needles, at $a=13$, while the jamming threshold decreases to a nonzero constant with a as a power law. The ratio of the two thresholds is nonmonotonic too—after initial growth it stabilizes for some values of a, and then it grows logarithmically. Whether the asymptotic value is equal to one or less is an interesting question. To answer it unequivocally is unfortunately beyond our computing power. The values of the correlation length exponent ν, for percolation, jamming thresholds, and the ratio of the two, do not depend on the length of the needles and they are, within the error bars, equal to those found elsewhere [12,13] for deposition of needles, rectangles, or squares.

[1] S.R. Broadbent and J.M. Hammersley, Cambridge Philos. Soc. **53**, 629 (1957).

[2] D. Stauffer, Physica A **242**, 1 (1997); D. Stauffer and A. Aharony, *Introduction to Percolation Theory* (Taylor and Francis, London, 1994).

[3] J.W. Evans, Rev. Mod. Phys. **65**, 1281 (1993).

[4] R.D. Vigil and R.M. Ziff, J. Chem. Phys. **91**, 2599 (1989).

[5] A.C. Balazs and I.R. Epstein, Biopolymers **23**, 1249 (1984).

[6] E.A. Boucher, Trans. Faraday Soc. **69**, 1839 (1973).

[7] J.J. Ramsden, Phys. Rev. Lett. **71**, 295 (1993).

[8] L. Finegold and J.T. Donnell, Nature (London) **278**, 443 (1979)

[9] P.J. Flory, Proc. R. Soc. London, Ser. A **234**, 73 (1956).

[10] H. Weber, W. Paul, and K. Binder, Phys. Rev. E **59**, 2168 (1999).

[11] C. Domb, E. Stoll, and T. Schneider, Contemp. Phys. **21**, 577 (1980).

[12] N. Vanderwalle, S. Galam, and M. Kramer, Eur. Phys. J. B **14**, 407 (2000).

[13] M. Nakamura, J. Phys. A **19**, 2345 (1986).